REGULAR ARTICLE

blood advances

Deleterious effect of bone marrow-resident macrophages on hematopoietic stem cells in response to total body irradiation

Marion Chalot,[1] Vilma Barroca,[1] Saiyirami Devanand,[1] Françoise Hoffschir,[1] Paul-Henri Romeo,[1] and Stéphanie G. Moreno[1]

[1]Université de Paris, Université Paris Saclay, INSERM-CEA, Stabilité Génétique Cellules Souches et Radiations, Laboratoire Réparation et Transcription dans les cellules Souches (LRTS), Institut de Radiobiologie Cellulaire et Moléculaire (iRCM), Institut de Biologie François Jacob (IBFJ), Direction de la Recherche Fondamentale (DRF), Fontenay-aux-Roses, France

Key Points

- After a 2 Gy TBI, NO produced by BM resident macrophages leads to formation of cytotoxic peroxynitrites in LT-HSCs.
- Depletion of BM resident macrophages or inhibition of NO production suppresses the cytotoxic effects of a 2 Gy TBI on LT-HSCs.

Bone marrow (BM) resident macrophages interact with a population of long-term hematopoietic stem cells (LT-HSCs) but their role on LT-HSC properties after stress is not well defined. Here, we show that a 2 Gy-total body irradiation (TBI)-mediated death of LT-HSCs is associated with increased percentages of LT-HSCs with reactive oxygen species (ROS) and of BM resident macrophages producing nitric oxide (NO), resulting in an increased percentage of LT-HSCs with endogenous cytotoxic peroxynitrites. Pharmacological or genetic depletion of BM resident macrophages impairs the radio-induced increases in the percentage of both ROS$^+$ LT-HSCs and peroxynitrite$^+$ LT-HSCs and results in a complete recovery of a functional pool of LT-HSCs. Finally, we show that after a 2 Gy-TBI, a specific decrease of NO production by BM resident macrophages improves the LT-HSC recovery, whereas an exogenous NO delivery decreases the LT-HSC compartment. Altogether, these results show that BM resident macrophages are involved in the response of LT-HSCs to a 2 Gy-TBI and suggest that regulation of NO production can be used to modulate some deleterious effects of a TBI on LT-HSCs.

Introduction

Total body irradiation (TBI) and localized radiation therapies are widely used in clinics. Despite their efficiency for bone marrow (BM) transplantation or to reduce tumor size, irradiation of healthy tissues present in the radiation field can lead to major deleterious side effects in patients. BM hematopoietic stem cells (HSCs) that ensure the renewal of mature blood cells lifelong are very sensitive to irradiation.[1-3] Indeed, a 2 Gy-TBI results in apoptosis, oxidative stress, and genomic instability in HSCs, decreasing their functionality and potentially leading to leukemia.[4-7] Thus, it is of prime importance to find out how to protect HSCs from the harmful effects of radiation.

HSCs are localized in complex cellular microenvironments called HSC niches, essential for HSC protection and regulation,[8,9] as they orchestrate HSC fate under homeostatic and stress conditions.[10] In homeostasis, N-CADHERIN$^+$ stromal cells support a highly quiescent HSC reserve,[11] NG2$^+$ periarteriolar cells maintain HSC in a dormant state,[12] CXCL12-abundant reticular (CAR) cells are essential to maintain a quiescent HSC pool,[13] and Akt-activated endothelial cells balance self-renewal and differentiation of HSCs.[14] BM resident macrophages (MΦ), localized in the mesenchymal niche, have a major role

Submitted 25 August 2021; accepted 29 January 2022; prepublished online on *Blood Advances* First Edition 31 January 2022; final version published online 15 March 2022. DOI 10.1182/bloodadvances.2021005983.

Sequencing data can be found in the Gene Expression Omnibus (www.ncbi.nlm.nih.gov/geo, accession number GSE189464). Please direct other inquiries to the corresponding author: stephanie.moreno@cea.fr.

The full-text version of this article contains a data supplement.

in the retention of HSCs in their niche, in their quiescence, and in their protection from oxidative stress.[15,16] In accordance, α-smooth muscle actin (SMA)$^+$ monocytes and macrophages expressing cyclooxygenase-2 (COX-2) maintain HSC quiescence by preserving low levels of reactive oxygen species (ROS).[17] In response to a stress, such as irradiation, this α-SMA$^+$ population further increases its COX-2 expression inducing prostaglandin E2 production to reduce the ROS level in HSCs and thus, maintains HSC pool integrity.[18] In the mesenchymal niche, BM resident MΦ expressing CD169 (also called sialoadhesin) are radioresistant and necessary for effective transplantation and hematopoietic reconstitution after lethal irradiation.[15,19] Therefore, BM resident MΦ are thought to be HSC protectors, particularly in response to stress.[20] However, CD169$^+$ MΦ may also have deleterious effects on HSCs as they can secrete proinflammatory cytokines[21] and produce chemokines that can recruit inflammatory monocytes. In accordance, a beneficial effect of an MΦ depletion has been shown in a model of severe aplastic anemia, as the absence of MΦ rescued HSC pool and reduced mortality in mice.[22]

Here, we study the effects of a 2 Gy-TBI on ROS, nitric oxide (NO), and peroxynitrite production by BM resident CD169$^+$ MΦ and long-term HSCs (LT-HSCs). Using pharmacological or genetic depletion of CD169$^+$ MΦ, we characterize the role of BM resident CD169$^+$ MΦ on LT-HSCs after a 2 Gy-TBI and show how the modulation of NO production can be used to control some deleterious effects of TBI on HSCs.

Methods

Mice

Eight- to 12-week-old C57BL/6 male mice were bred in our animal facility or purchased from Janvier Laboratory (CD45.2$^+$ C57BL/6JRj mice) or Charles River Laboratory (CD45.1$^+$ C57BL/6-Ly5.1 mice).

CD169-DTR homozygous mice (CD169$^{DTR/DTR}$, no. RBRC04395) were purchased from RIKEN BRC through the National Bio-Resource Project of the MEXT/AMED (Japan).[23,24] CD169-DTR heterozygous mice (CD169$^{DTR/+}$) were obtained by crossing CD169$^{DTR/DTR}$ with C57BL/6JRj mice.

Experimental procedures were performed in accordance with the European Community Council Directive (EC/2010/63) and were approved by our ethics committee (APAFIS#18486-2019011514438518v1). All mice were housed in our specific-pathogen-free-animal facility (registration number C9203202) and handled in compliance with the institutional guidelines and French Ministry of Agriculture's regulations.

Macrophage depletion

Chemical model. Clodronate-liposomes and phosphate-buffered saline (PBS)-liposomes were purchased from LIPOSOMA. C57BL/6 mice were anesthetized with isoflurane before IV retro-orbital injection. Clodronate-liposomes (200 μL) or PBS-liposomes (200 μL) were twice injected 40 and 16 hours before irradiation.[25]

Genetic model. CD169$^{DTR/+}$ and control C57BL/6 mice were injected intraperitoneally with a single dose of 10 μg/Kg Diphtheria Toxin (DT; Sigma-Aldrich #D0564)[15] 72 hours before irradiation.

Irradiation

Irradiations were performed on a GSR-D1 irradiator (γ-Service Medical GmbH company). It is a self-shielded irradiator with 4 ^{137}Cs sources for a total activity of 180.28 TBq (March 2014), which emits γ rays.

Statistical analysis

All statistical analysis was performed using Prism 8 (GraphPad Software). A 2-tailed Mann-Whitney *U* test was used to evaluate the statistical significance between the 2 groups. $P < .05$ was considered statistically significant.

Detailed methods are provided in the supplemental Appendix.

Results

A 2 Gy-TBI of mice induces production of NO by BM CD169$^+$ MΦ and of ROS by LT-HSCs, resulting in LT-HSCs containing cytotoxic peroxynitrites

In wild-type (WT) mice, a 2 Gy-TBI resulted in a first rapid decrease in the number of BM LT-HSCs followed by a partial recovery starting from 10 days after TBI (Figure 1A, left panel). These kinetics were associated with 2 waves of increased percentages of ROS$^+$ LT-HSCs. The first wave started 5 hours after TBI and ended 5 days after TBI, and the second wave started from 6 days after TBI and lasted up to 21 days after TBI (Figure 1A, right panel). In response to oxidative stress, MΦ produce NO through activation of the NO synthase 2 (iNOS).[26] In accordance, a 2 Gy-TBI led to a 2.5-fold increase of iNOS expression, mainly in resident CD169$^+$ MΦ (Figure 1B, left panels) as 4.3-fold more CD169$^+$ MΦ expressed iNOS compared with CD169^{neg} MΦ (supplemental Figure S1A, left panel). This increased expression of iNOS in CD169$^+$ MΦ was associated with the first wave of increased percentages of CD169$^+$ MΦ producing NO starting 5 hours after TBI and extending at least up to 2 days after TBI and with a second increase detected at day 10 after TBI (Figure 1B, right panel). Kinetics of total MΦ producing NO after a 2 Gy-TBI showed that CD169$^+$ MΦ were the main producers of NO (supplemental Figure S1B, right panel). These 2 increases of NO$^+$ CD169$^+$ MΦ were concomitant with the 2 waves of increased ROS$^+$ LT-HSCs observed after a 2 Gy-TBI (see Figure 1A).

NO by itself is a weak oxidant[27] but is extremely diffusible and can react with superoxide ions ($O2^-$) produced from ROS to form peroxynitrite anions ($OONO^-$) that are pathophysiologically relevant endogenous cytotoxins, highly toxic to cells[28] (Figure 1C). After a 2 Gy-TBI, 2 waves of increased percentage of LT-HSCs containing peroxynitrites were detected: one between 12 hours and 2 days after TBI and a second between 10 and 15 days after TBI (Figure 1D, left panel). These 2 waves were concomitant with increased percentages of NO$^+$ CD169$^+$ MΦ and ROS$^+$ LT-HSCs (see Figure 1A-B) and were associated with 2 waves of increased percentages of apoptotic LT-HSCs: a first one starting 5 hours after TBI and a second one starting 6 days after TBI (Figure 1D, right panel).

These results suggest that peroxynitrite production via the radio-induced ROS increase in LT-HSCs and the NO production by CD169$^+$ MΦ might account for the deleterious effects of a 2 Gy-TBI on LT-HSCs.

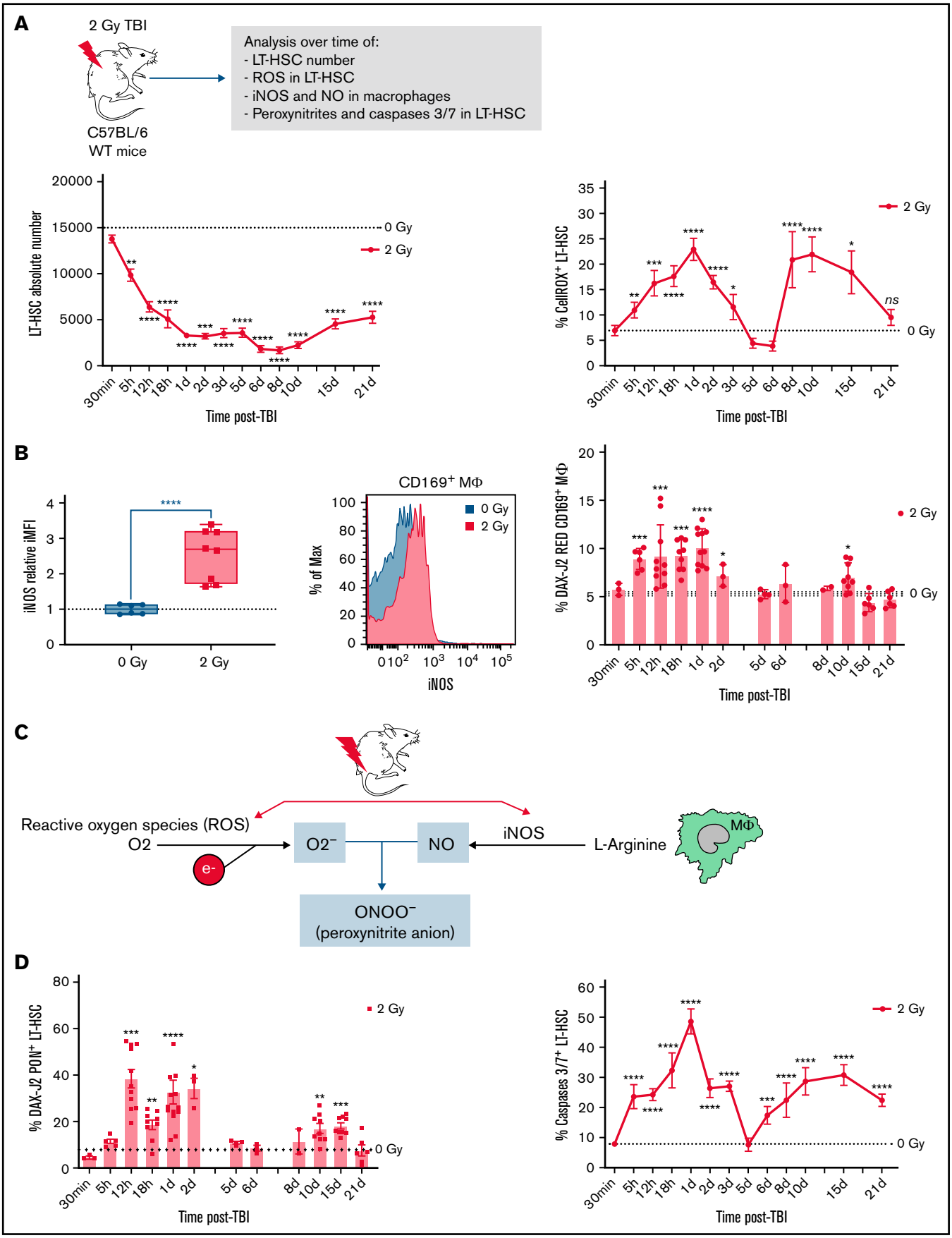
A
2 Gy TBI
C57BL/6
WT mice
Analysis over time of:
- LT-HSC number
- ROS in LT-HSC
- iNOS and NO in macrophages
- Peroxynitrites and caspases 3/7 in LT-HSC
LT-HSC absolute number
0 Gy
2 Gy
Time post-TBI
% CellROX+ LT-HSC
ns
B
iNOS relative iMFI
CD169+ MΦ
% of Max
iNOS
% DAX-J2 RED CD169+ MΦ
C
Reactive oxygen species (ROS)
O2
e-
O2−
NO
iNOS
L-Arginine
MΦ
ONOO−
(peroxynitrite anion)
D
% DAX-J2 PON+ LT-HSC
% Caspases 3/7+ LT-HSC

Figure 1.

Pharmacological or genetic depletion of CD169$^+$ MΦ preserves functional LT-HSCs after a 2 Gy-TBI

To characterize the role of resident CD169$^+$ MΦ on LT-HSCs after a 2 Gy-TBI, mice were previously treated with clodronate-liposomes (CLO-lipo) or PBS-liposomes (PBS-lipo) as a control (Figure 2A, upper scheme). Forty hours after CLO-lipo treatment, 86% of total BM MΦ were depleted, and the CD169$^+$ MΦ subpopulation was depleted by 98% (supplemental Figure S2A). As previously described,[15,29] lineage^{neg} Sca-1$^+$ c-kit$^+$ cells (LSKs) were mobilized 40 hours after CLO-lipo treatment (supplemental Figure S2B). This mobilization was not associated with a decreased number of LT-HSCs (Figure 2A, left panel), probably because BM LSKs have an increased proliferation (supplemental Figure S2C).

In contrast to PBS-lipo, CLO-lipo treatment delivered 40 hours before a 2 Gy-TBI did not result in an increased percentage of ROS$^+$ LT-HSCs 1 day after TBI (Figure 2A, upper right panel). The LT-HSC number, which decreased by 3.7-fold in PBS–lipo-treated mice, decreased only by 1.9-fold in CLO–lipo-treated mice (Figure 2A, lower left panel). This higher number of LT-HSCs in CLO–lipo-treated mice was associated with a lower percentage of apoptotic LT-HSCs and a higher percentage of LT-HSCs in *S*-G2-M (Figure 2A, middle and right panels). Thus, CLO-lipo treatment diminished the early deleterious effects of a 2 Gy-TBI on LT-HSCs. Five months after 2 Gy-TBI, CLO-lipo mice have recovered a normal number of total MΦ, but still have a decreased number of CD169$^+$ MΦ (supplemental Figure S2D) and have a normal number of LT-HSCs, whereas in PBS–lipo-treated mice, the number of LT-HSCs was 3-fold decreased (Figure 2B, left panel) and the percentage of LT-HSCs in apoptosis was 2.3-fold increased (Figure 2B, right panel).

As CLO-lipo depletes not only BM macrophages but most phagocytic cells, it can modulate the cell composition of the LT-HSC niches.[15,29,30] Thus, we studied by FACS analysis the effect of CLO-lipo on cells that are part of the LT-HSC niches (supplemental Figure S3A). Compared with PBS-lipo, a CLO-lipo treatment resulted, 40 hours later, in unchanged numbers of arteriolar endothelial cells (AECs) and sinusoidal endothelial cells (SECs), decreased numbers of osteoblasts (OBCs) and stromal CAR cells (3.6- and 2.4-fold, respectively), an increased number of stromal platelet-derived growth factor receptor Alpha (PDGFRa) cells (2.6-fold) and a dramatically decreased number of CD169$^+$ MΦ (45-fold) (supplemental Figure S3B). One day after a 2 Gy-TBI, PBS-lipo-treated mice showed a decreased number of CD169$^+$ MΦ (3.9-fold) and increased numbers of AECs and SECs (2- and 1.2-fold, respectively), whereas CLO-lipo-treated mice showed a further decrease of CD169$^+$ MΦ (2.3-fold), an increased number of SECs (1.6-fold), and decreased numbers of CAR and PDGFRa cells (1.4- and 2.4-fold, respectively) (supplemental Figure S3C). Thus, CLO-lipo treatment mostly decreased CD169$^+$ MΦ number but also slightly modified the number of other cells that are part of the LT-HSC niches.

Altogether, these results show that a CLO-lipo treatment delivered 40 hours before a 2 Gy-TBI protects LT-HSCs from the short- and long-term harmful effects due to irradiation and suggest a deleterious role of MΦ, in particular CD169$^+$ MΦ, in the effects of a 2 Gy-TBI on LT-HSCs.

To study the role of CD169$^+$ MΦ in the responses of LT-HSCs to a 2 Gy-TBI, we used a genetic mouse model to specifically deplete CD169$^+$ MΦ.[15,23] Three days after intraperitoneal injection of DT in CD169$^{DTR/+}$ mice, LSKs were mobilized in peripheral blood. This mobilization was not associated with a decreased number of LT-HSCs between non-irradiated WT and CD169$^{DTR/+}$ mice, probably because BM LSKs have an increased proliferation (supplemental Figure S4A).

In BM niches of CD169$^{DTR/+}$ mice, an unchanged number of AECs, a slight increased number of SECs (1.5-fold), slight decreased numbers of OBC, CAR, and PDGFRa cells (1.7-, 1.7-, and 1.6-fold, respectively), and a severe decrease of CD169$^+$ MΦ (35-fold) were found (supplemental Figures S4B,C). Analysis of these BM cells 1 day after a 2 Gy-TBI showed a decreased number of CD169$^+$ MΦ (2.5-fold) and an increased number of SEC (1.9-fold) in WT mice but did not show any modification of components of the niches in CD169$^{DTR/+}$ mice, except for the CD169$^+$ MΦ compartment, which was further decreased (2.3-fold) after TBI (supplemental Figure S4D). These results indicate that, except for CD169$^+$ MΦ, other cell populations found in the LT-HSC niches were less affected in CD169$^{DTR/+}$ mice than in the CLO-lipo model and suggest that the LT-HSC phenotype shown in this study was mainly due to the absence of CD169$^+$ MΦ.

After a 2 Gy-TBI performed 3 days after DT injection (Figure 2C), the BM cellularity followed the same kinetics in both WT and CD169$^{DTR/+}$ mice (supplemental Figure S4E). The first wave of increased percentages of apoptotic LT-HSCs occurred in WT mice and, at a lower extent, in CD169$^{DTR/+}$ mice, but the second wave of LT-HSC apoptosis, observed 6 days after TBI in WT mice, was not found in CD169$^{DTR/+}$ mice (Figure 2C, upper right panel). Compared with WT mice, the LT-HSC number in CD169$^{DTR/+}$ mice started to recover as soon as 5 days after TBI and reached a normal number from 15 days after TBI (Figure 2C, lower left panel). In WT mice, LT-HSCs were cycling 10 days after TBI (Figure 2C, lower right panel), but their number did not increase, suggesting that this higher proliferation was counterbalanced by the second wave of apoptosis (Figure 2C, upper right panel).

To characterize pathways regulating the second wave of apoptosis in WT mice, transcriptomic analysis of CD169$^{DTR/+}$ LT-HSCs vs WT LT-HSCs isolated 5 days after TBI (ie, just before the second waves of ROS and apoptosis occurring only in WT mice) was performed (supplemental Figure S5). This analysis showed that in

Figure 1. Decreased number of LT-HSCs and increased percentages of ROS$^+$ LT-HSCs, NO$^+$ CD169$^+$ macrophages (MΦ) and peroxynitrites$^+$ LT-HSCs after a 2 Gy-TBI. (A) Kinetics of LT-HSC number (left) and the percentage of ROS$^+$ LT-HSCs (right) in WT mice after a 2 Gy-TBI (n ≥ 3 mice for each time point). (B) Left: Increased iNOS expression in CD169$^+$ MΦ of WT mice 1 day after a 2 Gy-TBI (n = 3 independent experiments) and representative flow analysis of iNOS expression in CD169$^+$ MΦ 1 day after a 2 Gy-TBI. Right: Kinetics of CD169$^+$ MΦ producing NO in WT mice after a 2 Gy-TBI (n ≥ 3 mice for each time point). (C) Scheme describing the formation of peroxynitrites from radio-induced production of ROS and NO. (D) Kinetics of peroxynitrites$^+$ LT-HSCs (left) and of caspases 3/7$^+$ LT-HSCs (right) in WT mice after a 2 Gy-TBI (n ≥ 3 mice for each time point). Data are represented with mean ± SEM or min to max box-and-whisker; *$P < .05$, **$P < .01$, ***$P < .001$, ****$P < .0001$ (2-tailed Mann-Whitney *U* test).

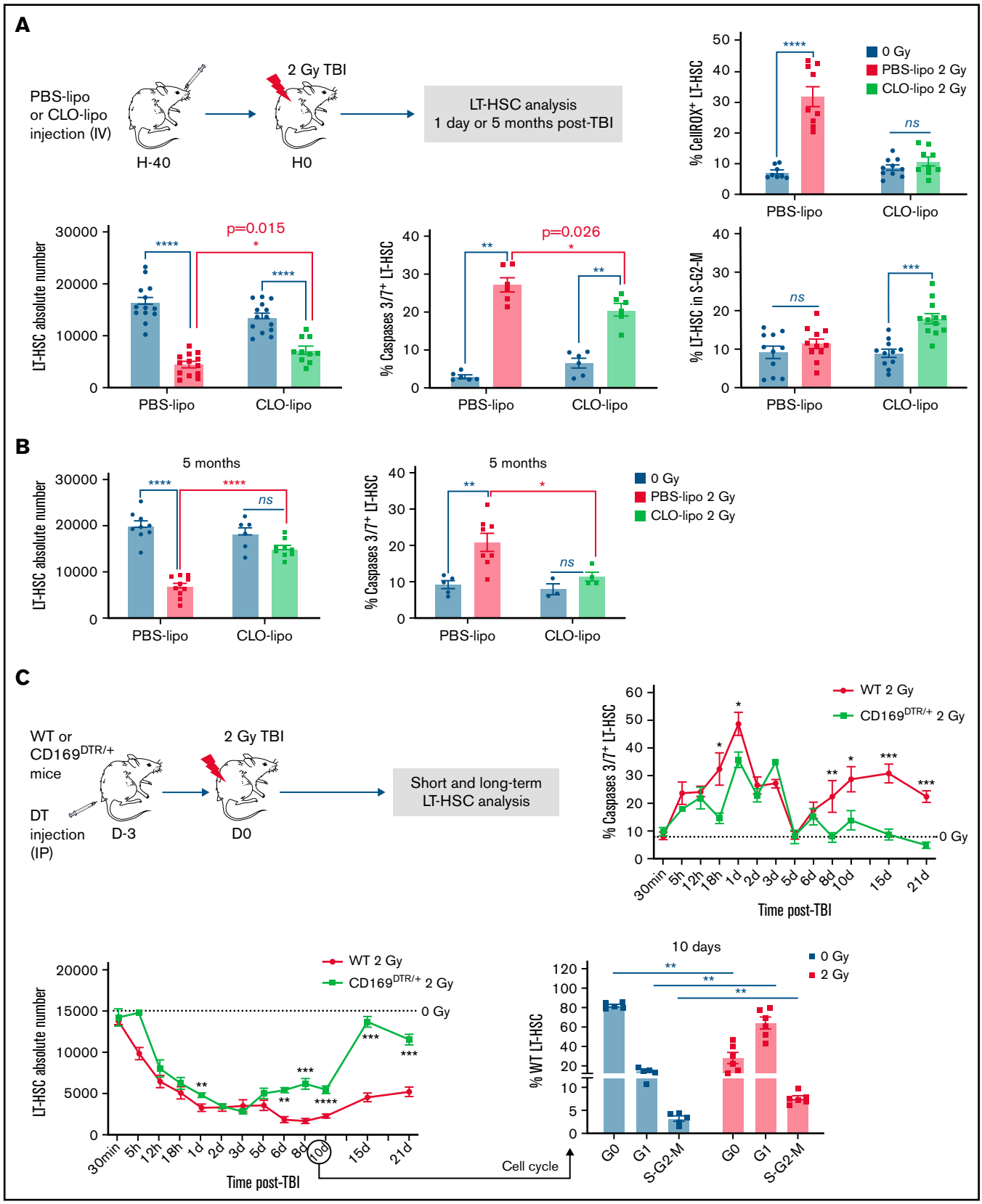

Figure 2. Effects of pharmacological or genetic depletion of CD169^{+} MΦ on LT-HSC fate short- and long-term after TBI. (A) Top: Scheme of the experimental protocol used for CLO-lipo treatment (left) and percentage of ROS+ LT-HSCs (right). Bottom: LT-HSC number (left), and percentages of caspases 3/7^{+} LT-HSCs (middle) and LT-HSCs in *S*-G2-M phases of the cell cycle (right) 1 day after a 2 Gy-TBI (n ≥ 5 mice). (B) LT-HSC number (left, n = 10 mice) and percentage of caspases

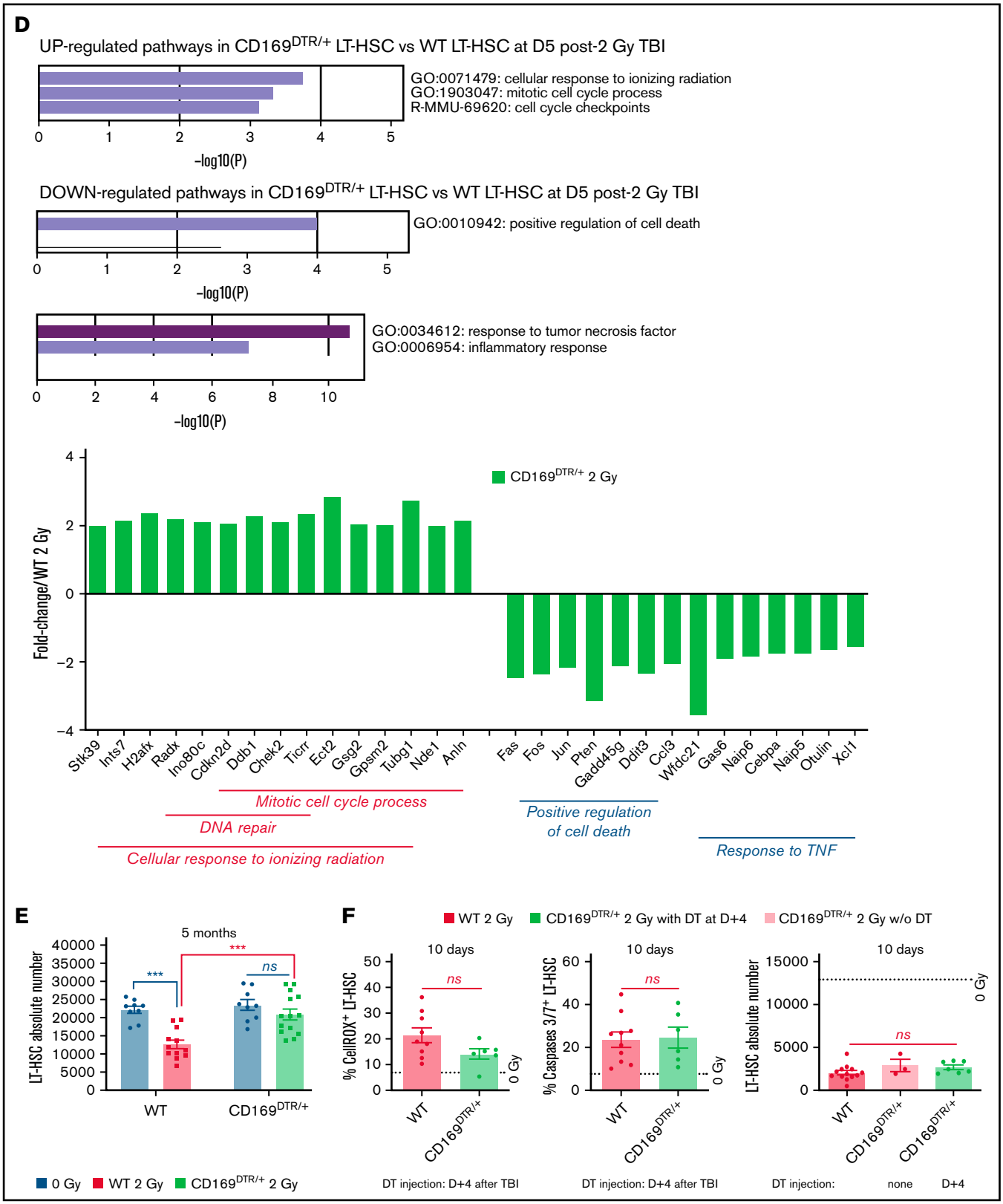

Figure 2 (continued) 3/7^{+} LT-HSCs (right, n ≥ 4 mice) 5 months after a 2 Gy-TBI. (C) Top: Scheme of the experimental protocol used for DT injection in WT and CD169$^{DTR/+}$ mice (left) and kinetics of caspases 3/7^{+} LT-HSC percentage (right). Bottom: Kinetics of LT-HSC number (left) in WT and CD169$^{DTR/+}$ mice after a 2 Gy-TBI. Cell cycle analysis of WT LT-HSCs 10 days after a 2 Gy-TBI (right) (n ≥3 mice for each time point). (D) Transcriptomic analysis of CD169$^{DTR/+}$ LT-HSCs vs WT LT-HSCs 5 days after a 2 Gy-TBI. Pathways up- and downregulated (top) and associated genes which are differentially expressed (bottom). (E) LT-HSC numbers in WT and CD169$^{DTR/+}$ mice 5 months after a 2 Gy-TBI (n ≥ 12 mice). (F) Percentages of ROS^{+} (left) or caspases 3/7^{+} (middle) LT-HSCs and number of LT-HSCs (right) 10 days after a 2 Gy-TBI in WT and CD169$^{DTR/+}$ mice DT-injected 4 days after TBI (n ≥ 3 mice). Data are represented with mean ± SEM; *$P < .05$, **$P < .01$, ***$P < .001$, ****$P < .0001$, *ns*: not statistically significant (2-tailed Mann-Whitney U test)

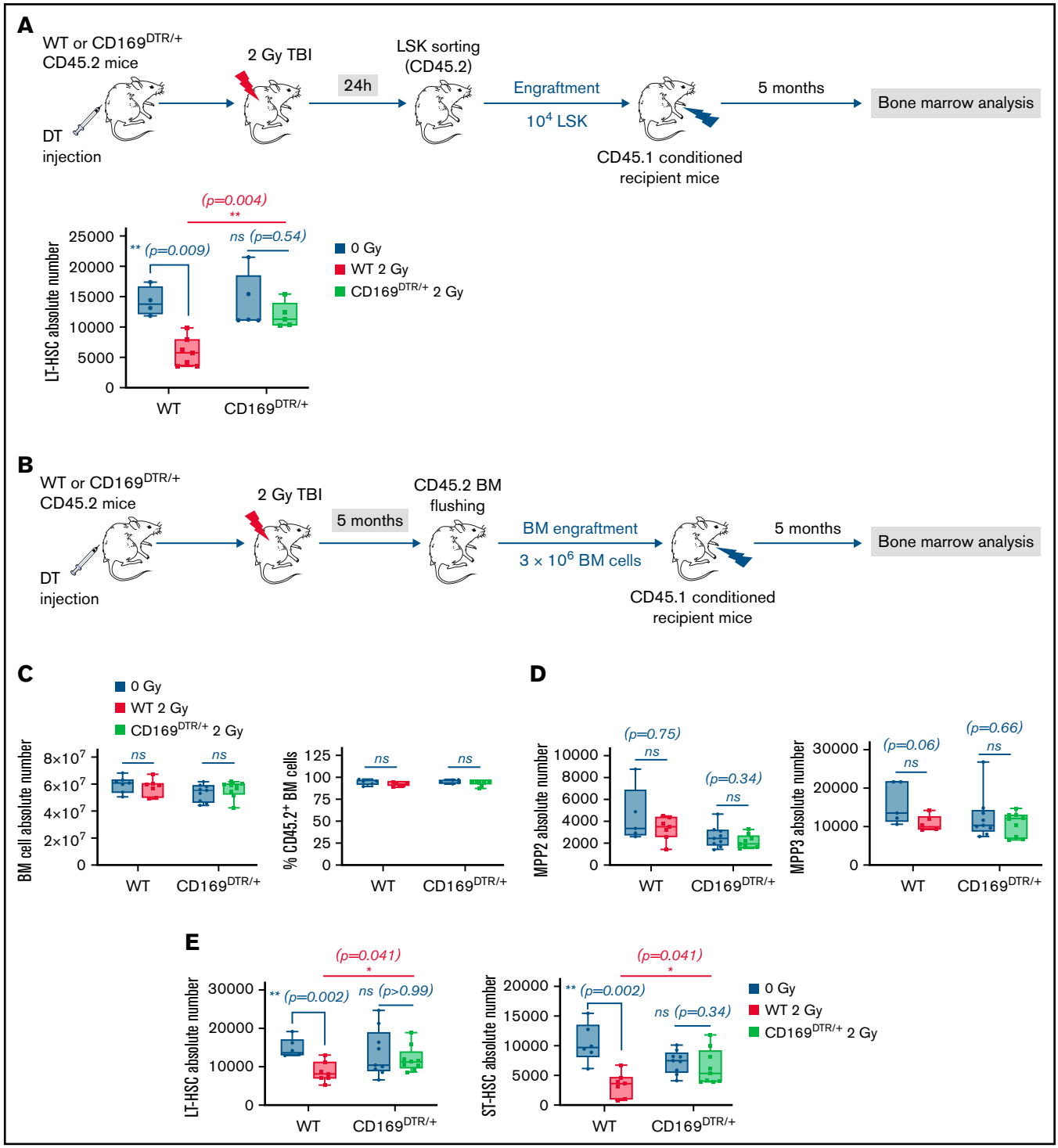

Figure 3. Effects of genetic depletion of CD169$^+$ MΦ on LT-HSC functionality after TBI. (A) Top: Scheme of the experimental protocol of LSK engraftment. Bottom: Number of donor LT-HSCs in recipient mice 5 months after LSK transplantation (n = 3 independent experiments). (B) Scheme of the experimental protocol of BM engraftment. (C) BM cellularity (left) and chimerism (right) in recipient mice 5 months after BM transplantation (n = 3 independent experiments). (D) Numbers of donor MPP2 (left) and MPP3 (right) in recipient mice 5 months after BM transplantation (n = 3 independent experiments). (E) Numbers of donor LT-HSCs (left) and ST-HSCs (right) in recipient mice 5 months after BM transplantation (n = 3 independent experiments). Data are represented with min to max box-and-whisker; *$P < .05$, **$P < .01$, *ns*: not statistically significant (2-tailed Mann-Whitney *U* test).

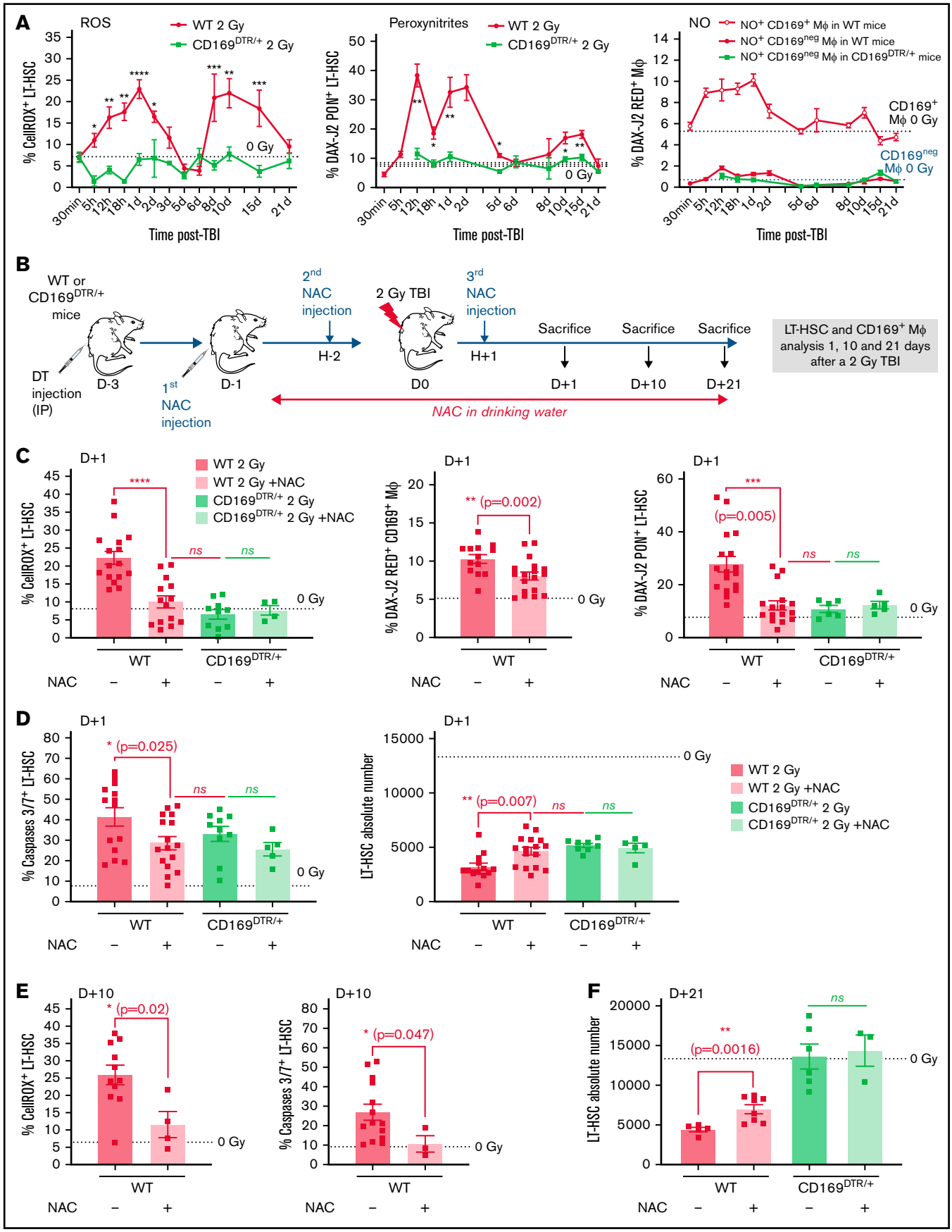
A
ROS
WT 2 Gy
CD169DTR/+ 2 Gy
% CellROX+ LT-HSC
0 Gy
Time post-TBI
Peroxynitrites
% DAX-J2 PON+ LT-HSC
NO
NO+ CD169+ Mϕ in WT mice
NO+ CD169neg Mϕ in WT mice
NO+ CD169neg Mϕ in CD169DTR/+ mice
% DAX-J2 RED+ Mϕ
CD169+ Mϕ 0 Gy
CD169neg Mϕ 0 Gy
B
WT or CD169DTR/+ mice
DT injection (IP)
D-3
1st NAC injection
D-1
2nd NAC injection
H-2
2 Gy TBI
D0
3rd NAC injection
H+1
Sacrifice
D+1
D+10
D+21
NAC in drinking water
LT-HSC and CD169+ Mϕ analysis 1, 10 and 21 days after a 2 Gy TBI
C
D+1
WT 2 Gy
WT 2 Gy +NAC
CD169DTR/+ 2 Gy
CD169DTR/+ 2 Gy +NAC
% CellROX+ LT-HSC
ns
0 Gy
WT
CD169DTR/+
NAC
% DAX-J2 RED+ CD169+ Mϕ
** (p=0.002)
% DAX-J2 PON+ LT-HSC
*** (p=0.005)
D
% Caspases 3/7+ LT-HSC
* (p=0.025)
LT-HSC absolute number
** (p=0.007)
E
D+10
* (p=0.02)
* (p=0.047)
F
D+21
** (p=0.0016)

Figure 4.

CD169$^{DTR/+}$ LT-HSCs, genes involved in DNA repair and cell cycle process in response to ionizing radiation were upregulated, and genes involved in cell death and response to TNFα were downregulated (Figure 2D).

Five months after a 2 Gy-TBI, CD169$^{DTR/+}$ mice, which still had a 2.3-fold decreased number of CD169^{+} MΦ (supplemental Figure S4F), recovered a normal LT-HSC number, whereas WT mice had a 1.7-fold decreased number of LT-HSCs (Figure 2E). To determine when CD169^{+} MΦ were involved in the deleterious effects of a 2 Gy-TBI on LT-HSCs, DT was injected into CD169$^{DTR/+}$ mice 4 days after a 2 Gy-TBI (ie, after the first wave of increased ROS^{+} LT-HSCs) (supplemental Figure S6A). Ten days after TBI, CD169^{+} MΦ have been efficiently depleted (supplemental Figure S6B), but this delayed CD169^{+} MΦ depletion did not suppress the second wave of ROS^{+} LT-HSCs, did not decrease the percentage of apoptotic LT-HSCs, and did not lead to an increased LT-HSC number after a 2 Gy-TBI (Figure 2F).

As a 2 Gy-TBI has effects on many organs, only 1 leg of WT and CD169$^{DTR/+}$ mice was irradiated at 2 Gy (supplemental Figure S7A). One day later, the LT-HSC number was 1.6-fold decreased in the irradiated leg of WT mice, and percentages of ROS^{+} LT-HSCs and apoptotic LT-HSCs were increased when compared with the non-irradiated leg. In the irradiated leg of CD169$^{DTR/+}$ mice, the decrease of the LT-HSC number was only 1.3-fold smaller, and percentages of ROS^{+} LT-HSCs and apoptotic LT-HSCs were similar to the ones observed in the non-irradiated leg (supplemental Figure S7B). These data suggest that CD169^{+} MΦ deficiency results in a local protection of LT-HSCs against the deleterious effects of a 2 Gy irradiation.

To characterize the role of CD169^{+} MΦ in the short-term functions of LT-HSCs after a 2 Gy-TBI, LSK from WT or CD169$^{DTR/+}$ mice were sorted 24 hours after TBI and transplanted into conditioned recipient mice. Five months later, recipient mice that were transplanted with LSK from irradiated WT donor mice had a decreased number of LT-HSCs, whereas recipient mice transplanted with LSK from irradiated CD169$^{DTR/+}$ donor mice had a normal number of LT-HSCs (Figure 3A).

We also characterized the role of CD169^{+} MΦ in the long-term functions of LT-HSCs 5 months after a 2 Gy-TBI. BM from WT or CD169$^{DTR/+}$ mice was harvested 5 months after a 2 Gy-TBI and transplanted into conditioned recipient mice. BM from recipient mice was then analyzed 5 months later (Figure 3B). BM cellularity and chimerism (Figure 3C), myeloid-biased MPP2 and MPP3 numbers associated with inflammation (Figure 3D), and mature cell numbers (data not shown) were similar in the 4 groups of mice. However, whereas recipient mice that were transplanted with BM from irradiated WT donor mice had decreased numbers of LT- and ST-HSCs, recipient mice transplanted with BM from irradiated CD169$^{DTR/+}$ donor mice had normal numbers of LT- and ST-HSCs (Figure 3E).

Altogether, these data show that CD169^{+} MΦ deficiency results in early protection of functional LT-HSCs against the deleterious effects of a 2 Gy irradiation.

The CD169^{+} MΦ depletion suppressed the radio-induced increase of ROS^{+} LT-HSCs and could be partially mimicked by a NAC treatment

A 2 Gy-TBI of CD169$^{DTR/+}$ mice did not result in any increased percentage of ROS^{+} LT-HSCs nor percentage of LT-HSCs containing peroxynitrites over time (Figure 4A, left, middle panels). Of note, MΦ present in CD169$^{DTR/+}$ mice did not produce radio-induced NO (Figure 4A, right panel).

To prevent the radio-induced increase of ROS due to TBI, WT mice were treated with N-acetyl-L-cysteine (NAC), a ROS scavenger,[31] before and after a 2 Gy-TBI (Figure 4B). This treatment resulted in a 2.2-fold reduced percentage of ROS^{+} LT-HSCs 1 day after TBI (ie, similar to the percentage found in irradiated CD169$^{DTR/+}$ mice) (Figure 4C, left panel). In 2 Gy-irradiated WT mice, NAC treatment also decreased by 1.3-fold the percentage of CD169^{+} MΦ producing NO (Figure 4C, middle panel) and by 2.3-fold the percentage of LT-HSCs with peroxynitrites (Figure 4C, right panel). These lower percentages were associated with a 1.4-fold decreased percentage of radio-induced apoptotic LT-HSCs (Figure 4D, left panel) and with a 1.5-fold increase of the LT-HSC number (Figure 4D, right panel). Ten days after TBI, the percentage of ROS^{+} LT-HSCs was still 2.2-fold decreased by NAC treatment, and no increase in the percentage of radio-induced apoptotic LT-HSCs (Figure 4E) was observed, suggesting the abolishment of a second wave of apoptosis. Finally, 21 days after TBI, the LT-HSC number was 1.6-fold increased in WT mice treated with NAC but was significantly decreased compared with irradiated CD169$^{DTR/+}$ mice or to non-irradiated mice (Figure 4F).

Altogether, these results suggest that in WT mice, the first wave of apoptosis in LT-HSCs is only partially ROS-dependent as a NAC treatment did not completely suppress apoptosis 1 day post-TBI. In contrast, the second wave of apoptosis in LT-HSCs is ROS-dependent as, 10 days after TBI, NAC treatment suppresses this second wave of apoptosis. In CD169$^{DTR/+}$ mice, the first wave of apoptosis is ROS-independent as there is no increase of ROS^{+} LT-HSCs after TBI in these mice (Figure 4A, left panel) and as a NAC treatment did not decrease LT-HSC apoptosis (Figure 4D, left panel).

Modulation of NO production regulates LT-HSC recovery after a 2 Gy-TBI

To determine the role of NO in the early effects of a 2 Gy-TBI on LT-HSCs, WT mice were treated with 1400W, a selective inhibitor

Figure 4. Effects of CD169^{+} MΦ depletion or NAC treatment on the radio-induced increases of the percentages of ROS^{+} and peroxynitrite^{+} LT-HSCs. (A) Kinetics of percentages of ROS^{+} LT-HSCs (left) and peroxynitrite^{+} LT-HSCs (middle) in WT and CD169$^{DTR/+}$ mice. Kinetics of percentages of CD169^{+} MΦ and CD169^{neg} MΦ producing NO (right) in WT and CD169$^{DTR/+}$ mice (n ≥ 3 mice for each time point). (B) Scheme of the experimental protocol for NAC treatment of WT or CD169$^{DTR/+}$ mice. (C) Percentages of ROS^{+} LT-HSCs (left), of CD169^{+} MΦ producing NO (middle), and of peroxynitrite^{+} LT-HSCs (right) 1 day after a 2 Gy-TBI in WT and CD169$^{DTR/+}$ mice treated or not with NAC. (D) Percentage of caspases 3/7^{+} LT-HSCs (left) and number of LT-HSCs (right) 1 day after a 2 Gy-TBI in WT and CD169$^{DTR/+}$ mice treated or not with NAC (n ≥ 5 mice for each time point). (E) Percentages of ROS^{+} LT-HSCs (left) and caspases 3/7^{+} LT-HSCs (right) 10 days after a 2 Gy-TBI in WT mice treated or not with NAC (n ≥ 4 mice). (F) LT-HSC number 21 days after a 2 Gy-TBI in WT and CD169$^{DTR/+}$ mice treated or not with NAC (n ≥ 4 mice for each time point). Data are represented with mean ± SEM; *$P < .05$, **$P < .01$, ***$P < .001$, ****$P < .0001$, *ns*: not statistically significant (2-tailed Mann-Whitney *U* test).

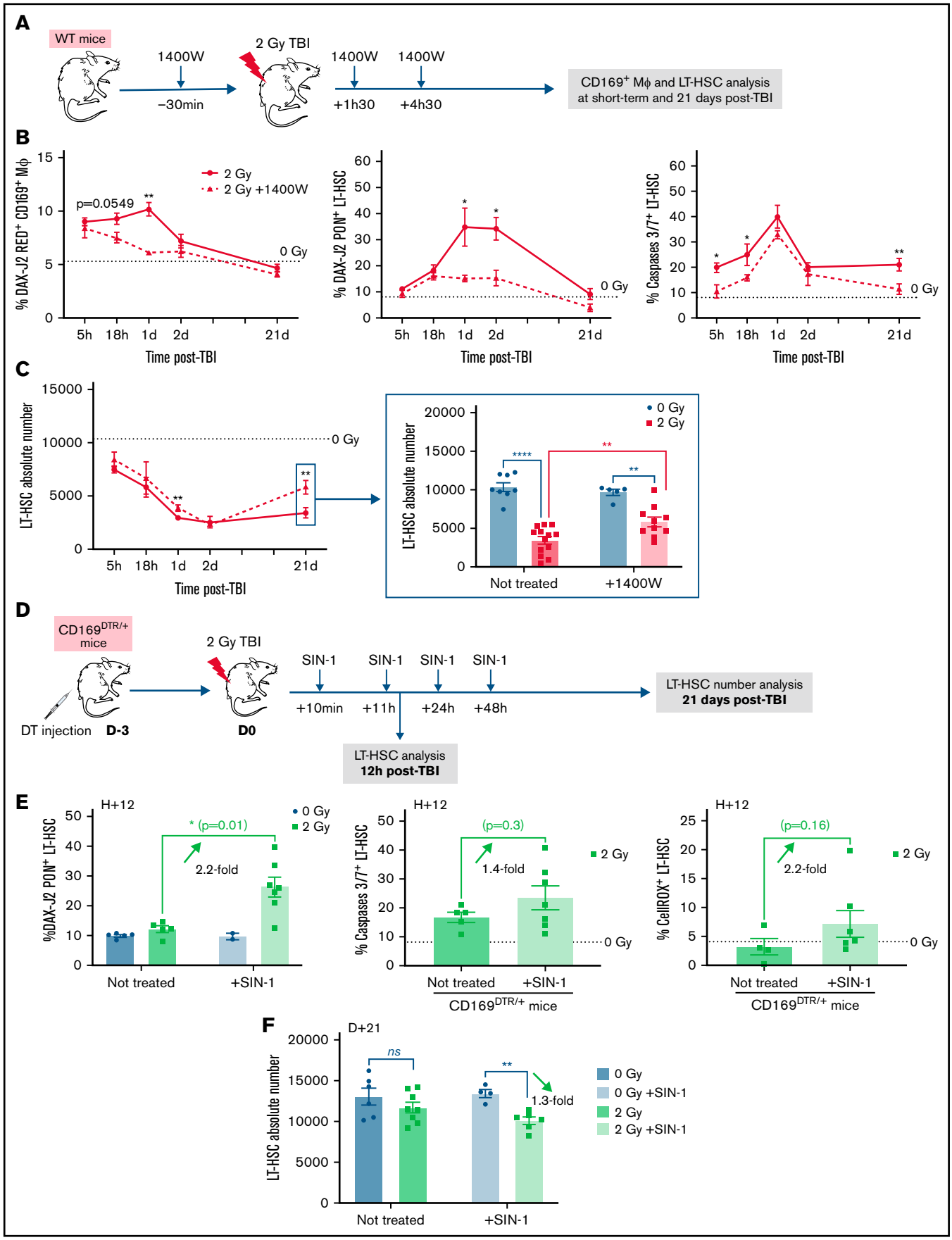
A
WT mice
1400W
−30min
2 Gy TBI
1400W
+1h30
1400W
+4h30
CD169+ Mϕ and LT-HSC analysis
at short-term and 21 days post-TBI
B
% DAX-J2 RED+ CD169+ Mϕ
2 Gy
2 Gy +1400W
p=0.0549
0 Gy
% DAX-J2 PON+ LT-HSC
% Caspases 3/7+ LT-HSC
5h 18h 1d 2d 21d
Time post-TBI
C
LT-HSC absolute number
0 Gy
Not treated
+1400W
D
CD169DTR/+ mice
DT injection D-3
2 Gy TBI
D0
SIN-1
+10min +11h +24h +48h
LT-HSC number analysis
21 days post-TBI
LT-HSC analysis
12h post-TBI
E
H+12
%DAX-J2 PON+ LT-HSC
* (p=0.01)
2.2-fold
Not treated
+SIN-1
% Caspases 3/7+ LT-HSC
(p=0.3)
1.4-fold
CD169DTR/+ mice
% CellROX+ LT-HSC
(p=0.16)
2.2-fold
F
D+21
ns
1.3-fold
0 Gy
0 Gy +SIN-1
2 Gy
2 Gy +SIN-1

Figure 5.

of iNOS,[32,33] 30 minutes before and 1 hour and 30 minutes and 4 hours and 30 minutes after a 2 Gy-TBI (Figure 5A). In 1400W-treated irradiated mice, a progressive decrease in the percentage of NO^+ $CD169^+$ MΦ was found to finally reach levels similar to those observed in non-irradiated mice (Figure 5B, left panel). This reduced NO production was associated with decreased percentages of peroxynitrite$^+$ LT-HSCs and of apoptotic LT-HSCs after TBI (Figure 5B, middle and right panels) and resulted in an increased number of LT-HSCs at 21 days post-TBI (Figure 5C), indicating that an early inhibition of NO production led to a partial rescue of the LT-HSC pool.

Conversely, to determine if increased NO levels were involved in the decreased number of LT-HSCs after TBI, DT-injected $CD169^{DTR/+}$ mice were inoculated with the NO donor SIN-1[34,35] 10 minutes, 11 hours, 24 hours, and 48 hours after a 2 Gy-TBI (Figure 5D). Twelve hours post-TBI, increased percentages of peroxynitrite$^+$ LT-HSCs, apoptotic LT-HSCs, and ROS^+ LT-HSCs were found in SIN-1-treated $CD169^{DTR/+}$ mice (Figure 5E). Finally, 21 days after TBI, the LT-HSC number was significantly decreased in SIN-1-treated $CD169^{DTR/+}$ mice compared with non-irradiated ones (Figure 5F).

Altogether, these results suggest a critical role of NO in the fate of LT-HSCs after a 2 Gy-TBI.

Discussion

In this study, we show that in response to a 2 Gy-TBI, BM resident $CD169^+$ MΦ have a detrimental effect on LT-HSCs. Their absence at the time of irradiation decreased the radio-induced ROS^+ LT-HSCs and apoptotic LT-HSCs and allowed a complete recovery of functional LT-HSCs long-time after TBI. In the irradiated heart, $CD68^+$ MΦ that are recruited after irradiation are responsible for cardiac physiological alterations,[36] and in the irradiated lung, the radio-induced fibrosis is accounted for recruited interstitial MΦ but not for resident alveolar MΦ.[37] These studies suggest that inflammatory recruited MΦ account for some detrimental effects of irradiation and that tissue-resident MΦ are protective sentinels restoring tissue homeostasis after injury.[38] In contrast, our results show that in the irradiated BM, the resident MΦ are involved in the radio-induced toxicity. This is consistent with studies showing that resident MΦ can induce tissue toxicity in the context of diseases such as obesity or atherosclerosis[39,40] or acute inflammation models.[41,42]

After a 2 Gy-TBI, the percentage of $CD169^+$ MΦ producing NO increased rapidly via an enhanced expression of iNOS, a property of proinflammatory MΦ,[26,43] suggesting that resident BM $CD169^+$ MΦ might acquire a proinflammatory M1 phenotype in response to a 2 Gy-TBI. This increase of NO^+ $CD169^+$ MΦ is associated with an increased percentage of LT-HSCs containing peroxynitrites. Peroxynitrites, whose formation results from a chemical reaction between NO and superoxide anions,[27] are cytotoxic endogenous oxidants. This cytotoxicity is accounted for by mechanisms such as (i) inactivation of superoxide dismutase enzymes,[44-46] (ii) induction of DNA damages,[47] and (iii) abnormal mitochondrial function leading to secondary ROS formation.[48] How peroxynitrites are involved in LT-HSC apoptosis is still unknown.

Although NAC treatment decreased both percentages of NO^+ MΦ and peroxynitrite$^+$ LT-HSCs after a 2 Gy-TBI, it did not totally suppress the first wave of LT-HSC apoptosis but lowered it to the one found in $CD169^{DTR/+}$ mice. In contrast, NAC treatment prevented the second wave of LT-HSC apoptosis in WT mice. These results indicated that early effects of a 2 Gy-TBI on LT-HSCs involved both ROS-independent and ROS-dependent apoptosis and that the second wave of apoptosis was only ROS-dependent. Here, we demonstrated that the ROS-dependent apoptosis is mainly due to peroxynitrite formation as a result of the combination of ROS produced by LT-HSCs with NO produced by $CD169^+$ MΦ. The ROS-independent apoptosis can be due to a mitochondrial dysfunction that leads to caspase 3 activation[49-51] as we found a 2.6-fold increase of the percentage of LT-HSCs with mitochondrial ROS 1 day after a 2 Gy-TBI (our unpublished data).

In accordance with the phenotypes observed, transcriptomic analysis of LT-HSCs, harvested before the second waves of ROS and apoptosis, showed, in $CD169^{DTR/+}$ LT-HSCs, an increased expression of genes involved in cell proliferation and in response to ionizing radiation and a decreased expression of genes involved in apoptosis, such as *Ddit3*, *Jun*, and *Fos*, and involved in response to TNFα. *Ddit3*, *Jun*, and *Fos* expressions are increased in response to endoplasmic reticulum (ER) stress and are associated with ROS production by mitochondria and apoptosis.[52,53] The decreased expression of these genes in $CD169^{DTR/+}$ LT-HSC suggests that, in WT mice, the first wave of radio-induced ROS might induce an extended activation of *Ddit3* due to ER stress, leading to the second wave of ROS. TNFα is produced by MΦ in stress conditions[54] and has a major role in mitochondrial-mediated cell death.[55] In addition, in vivo administration of TNFα in WT mice results in a decreased long-term repopulating activity of HSCs.[56] Our transcriptomic analysis showed a decreased expression of genes involved in response to TNFα in $CD169^{DTR/+}$ LT-HSCs, suggesting that, after a 2 Gy-TBI of WT mice, TNFα is rapidly secreted by $CD169^+$ MΦ and leads to mitochondrial and ER dysfunctions[57] in LT-HSCs that result in ROS and apoptosis. In accordance with the role of this early secretion of TNFα by $CD169^+$ MΦ, we showed that $CD169^+$ MΦ depletion after the first wave of ROS did not abolish the second wave of ROS.

Treatment of WT mice with the iNOS inhibitor 1400W, which leads to a specific inhibition of NO produced by MΦ,[58] led to decreased percentages of both peroxynitrite$^+$ LT-HSCs and apoptotic LT-HSCs and to a better recovery of LT-HSC number 21 days post-TBI. A 1400W treatment combined with radiotherapy

Figure 5. Modulation of NO production regulates LT-HSC recovery after a 2 Gy-TBI. (A) Scheme of the experimental protocol for the treatment of WT mice with the iNOS inhibitor (1400W) before and after a 2 Gy-TBI. (B) Kinetics of percentages of NO^+ $CD169^+$ MΦ (left), peroxynitrites$^+$ LT-HSCs (middle), and caspases $3/7^+$ LT-HSCs (right) in WT mice treated or not with 1400W ($n \geq 4$ mice for each time point). (C) Kinetics of LT-HSC number in WT mice treated or not with 1400W ($n \geq 4$ mice for each time point). (D) Scheme of the experimental protocol for the treatment of $CD169^{DTR/+}$ mice with the NO donor (SIN-1) after a 2 Gy-TBI. (E) Percentages of peroxynitrites$^+$ LT-HSCs (left), caspases $3/7^+$ LT-HSCs (middle), and ROS^+ LT-HSCs (right) 12 hours after a 2 Gy-TBI, in $CD169^{DTR/+}$ mice treated or not with SIN-1 ($n \geq 5$ mice). (F) LT-HSC number 21 days after a 2 Gy-TBI, in $CD169^{DTR/+}$ mice treated or not with SIN-1 ($n \geq 6$ mice). Data are represented with mean ± SEM; $^*P < .05$, $^{**}P < .01$, $^{****}P < .0001$, *ns*: not statistically significant (2-tailed Mann-Whitney *U* test).

increases survival and delays or suppresses tumor growth in the pancreas, lung, and breast cancer.[59,60] Our results strengthened its use in cancer treatment as we showed that 1400W treatment also protected LT-HSCs from potentially deleterious effects of radiotherapy. In contrast, the use of SIN-1, a NO donor, led to a decreased number of the LT-HSCs in CD169$^{DTR/+}$ mice 21 days after irradiation, strengthening the association between the presence of environmental NO and the harmful effect of irradiation on LT-HSCs. Interestingly, a SIN-1 treatment to 2 Gy-irradiated WT mice further decreased LT-HSC number 21 days post-TBI (our unpublished data), suggesting NO delivery as a potential way to reduce the radiation dose in conditioning regimens used in medical myeloablation.[61]

Altogether, this study characterized an unexpected role of BM CD169^{+} macrophages in the response of LT-HSCs to a 2 Gy-TBI and suggested that modulation of NO production might be an interesting tool in the medical use of ionizing radiation.

Acknowledgments

The authors thank the veterinary staff of Institute S. Vincent-Naulleau and V. Neuville and Animalliance for taking care of the mice; N. Dechamps for cell sorting; and V. Menard for assistance with irradiation. The authors also thank Kenji Kohno and Masato Tanaka for acceptance of the use of CD169$^{DTR/DTR}$ mice; F. Ferri and D. Lewandowski for help and support; and N. Gault for help and critical reading of the manuscript.

This work was supported by the IRBIO/CEA program and INSERM. The fourth year of M.C.'s thesis was funded by the Medical Research Foundation (FRM).

Authorship

Contribution: M.C. performed all experiments and wrote the manuscript; V.B., S.D., and F.H. provided experimental assistance; P.-H.R. wrote the manuscript; and S.G.M. designed, supervised, and performed all experiments, prepared figures, and wrote the manuscript.

Conflict-of-interest disclosure: The authors declare no competing financial interests.

ORCID profile: S.G.M., 0000-0002-5019-0856.

Correspondence: Stéphanie G. Moreno, iRCM/LRTS, CEA Fontenay-aux-roses, 18 route du Panorama, 92260 Fontenay-aux-roses, France; e-mail: stephanie.moreno@cea.fr; and Paul-Henri Romeo, iRCM/LRTS, CEA Fontenay-aux-roses, 18 route du Panorama, 92260 Fontenay-aux-roses, France; e-mail: paul-henri.romeo@cea.fr.

References

1. Green DE, Rubin CT. Consequences of irradiation on bone and marrow phenotypes, and its relation to disruption of hematopoietic precursors. *Bone.* 2014;63:87-94.
2. Rodrigues-Moreira S, Moreno SG, Ghinatti G, et al. Low-dose irradiation promotes persistent oxidative stress and decreases self-renewal in hematopoietic stem cells. *Cell Rep.* 2017;20(13):3199-3211.
3. Willey JS, Lloyd SAJ, Robbins ME, et al. Early increase in osteoclast number in mice after whole-body irradiation with 2 Gy X rays. *Radiat Res.* 2008;170(3):388-392.
4. Guo C-Y, Luo L, Urata Y, et al. Sensitivity and dose dependency of radiation-induced injury in hematopoietic stem/progenitor cells in mice. *Sci Rep.* 2015;5(1):8055.
5. Lu Y, Hu M, Zhang Z, Qi Y, Wang J. The regulation of hematopoietic stem cell fate in the context of radiation. *Radiat. Med. Prot.* 2020;1(1):31-34.
6. Mohrin M, Bourke E, Alexander D, et al. Hematopoietic stem cell quiescence promotes error-prone DNA repair and mutagenesis. *Cell Stem Cell.* 2010;7(2):174-185.
7. Shao L, Luo Y, Zhou D. Hematopoietic stem cell injury induced by ionizing radiation. *Antioxid Redox Signal.* 2014;20(9):1447-1462.
8. Mendelson A, Frenette PS. Hematopoietic stem cell niche maintenance during homeostasis and regeneration. *Nat Med.* 2014;20(8):833-846.
9. Wei Q, Frenette PS. Niches for hematopoietic stem cells and their progeny. *Immunity.* 2018;48(4):632-648.
10. Morrison SJ, Scadden DT. The bone marrow niche for haematopoietic stem cells. *Nature.* 2014;505(7483):327-334.
11. Zhao M, Tao F, Venkatraman A, et al. N-cadherin-expressing bone and marrow stromal progenitor cells maintain reserve hematopoietic stem cells. *Cell Rep.* 2019;26(3):652-669.e6.
12. Kunisaki Y, Bruns I, Scheiermann C, et al. Arteriolar niches maintain haematopoietic stem cell quiescence. *Nature.* 2013;502(7473):637-643.
13. Sugiyama T, Kohara H, Noda M, Nagasawa T. Maintenance of the hematopoietic stem cell pool by CXCL12-CXCR4 chemokine signaling in bone marrow stromal cell niches. *Immunity.* 2006;25(6):977-988.
14. Kobayashi H, Butler JM, O'Donnell R, et al. Angiocrine factors from Akt-activated endothelial cells balance self-renewal and differentiation of haematopoietic stem cells. *Nat Cell Biol.* 2010;12(11):1046-1056.
15. Chow A, Lucas D, Hidalgo A, et al. Bone marrow CD169^{+} macrophages promote the retention of hematopoietic stem and progenitor cells in the mesenchymal stem cell niche. *J Exp Med.* 2011;208(2):261-271.
16. Hur J, Choi J-I, Lee H, et al. CD82/KAI1 maintains the dormancy of long-term hematopoietic stem cells through interaction with DARC-expressing macrophages. *Cell Stem Cell.* 2016;18(4):508-521.
17. Ludin A, Itkin T, Gur-Cohen S, et al. Monocytes-macrophages that express α-smooth muscle actin preserve primitive hematopoietic cells in the bone marrow. *Nat Immunol.* 2012;13(11):1072-1082.

18. Ludin A, Gur-Cohen S, Golan K, et al. Reactive oxygen species regulate hematopoietic stem cell self-renewal, migration and development, as well as their bone marrow microenvironment. *Antioxid Redox Signal.* 2014;21(11):1605-1619.

19. Kaur S, Raggatt LJ, Millard SM, et al. Self-repopulating recipient bone marrow resident macrophages promote long-term hematopoietic stem cell engraftment. *Blood.* 2018;132(7):735-749.

20. Seyfried AN, Maloney JM, MacNamara KC. Macrophages orchestrate hematopoietic programs and regulate HSC function during inflammatory stress. *Front Immunol.* 2020;11:1499.

21. Li Q, Wang D, Hao S, et al. CD169 expressing macrophage, a key subset in mesenteric lymph nodes promotes mucosal inflammation in dextran sulfate sodium-induced colitis. *Front Immunol.* 2017;8:669.

22. McCabe A, Smith JNP, Costello A, Maloney J, Katikaneni D, MacNamara KC. Hematopoietic stem cell loss and hematopoietic failure in severe aplastic anemia is driven by macrophages and aberrant podoplanin expression. *Haematologica.* 2018;103(9):1451-1461.

23. Miyake Y, Asano K, Kaise H, Uemura M, Nakayama M, Tanaka M. Critical role of macrophages in the marginal zone in the suppression of immune responses to apoptotic cell-associated antigens. *J Clin Invest.* 2007;117(8):2268-2278.

24. Saito M, Iwawaki T, Taya C, et al. Diphtheria toxin receptor-mediated conditional and targeted cell ablation in transgenic mice. *Nat Biotechnol.* 2001;19(8):746-750.

25. Moreno SG. Depleting macrophages in vivo with clodronate-liposomes. *Methods Mol Biol.* 2018;1784:259-262.

26. Narang H, Krishna M. Inhibition of radiation induced nitration by curcumin and nicotinamide in mouse macrophages. *Mol Cell Biochem.* 2005; 276(1-2):7-13.

27. Radi R. Oxygen radicals, nitric oxide, and peroxynitrite: redox pathways in molecular medicine. *Proc Natl Acad Sci USA.* 2018;115(23):5839-5848.

28. Pacher P, Beckman JS, Liaudet L. Nitric oxide and peroxynitrite in health and disease. *Physiol Rev.* 2007;87(1):315-424.

29. Winkler IG, Sims NA, Pettit AR, et al. Bone marrow macrophages maintain hematopoietic stem cell (HSC) niches and their depletion mobilizes HSCs. *Blood.* 2010;116(23):4815-4828.

30. Batoon L, Millard SM, Wullschleger ME, et al. $CD169^{+}$ macrophages are critical for osteoblast maintenance and promote intramembranous and endochondral ossification during bone repair. *Biomaterials.* 2019;196:51-66.

31. Wang Y, Liu L, Pazhanisamy SK, Li H, Meng A, Zhou D. Total body irradiation causes residual bone marrow injury by induction of persistent oxidative stress in murine hematopoietic stem cells. *Free Radic Biol Med.* 2010;48(2):348-356.

32. Atochina-Vasserman EN, Beers MF, Kadire H, et al. Selective inhibition of inducible NO synthase activity in vivo reverses inflammatory abnormalities in surfactant protein D-deficient mice. *J. Immunol.* 2007;179(12):8090-8097.

33. Garvey EP, Oplinger JA, Furfine ES, et al. 1400W is a slow, tight binding, and highly selective inhibitor of inducible nitric-oxide synthase in vitro and in vivo. *J Biol Chem.* 1997;272(8):4959-4963.

34. Singh RJ, Hogg N, Joseph J, Konorev E, Kalyanaraman B. The peroxynitrite generator, SIN-1, becomes a nitric oxide donor in the presence of electron acceptors. *Arch Biochem Biophys.* 1999;361(2):331-339.

35. Xu L-Y, Yang J-S, Link H, Xiao B-G. SIN-1, a nitric oxide donor, ameliorates experimental allergic encephalomyelitis in Lewis rats in the incipient phase: the importance of the time window. *J Immunol.* 2001;166(9):5810-5816.

36. Monceau V, Meziani L, Strup-Perrot C, et al. Enhanced sensitivity to low dose irradiation of ApoE−/− mice mediated by early pro-inflammatory profile and delayed activation of the TGFβ1 cascade involved in fibrogenesis. *PLoS One.* 2013;8(2):e57052.

37. Meziani L, Mondini M, Petit B, et al. CSF1R inhibition prevents radiation pulmonary fibrosis by depletion of interstitial macrophages. *Eur Respir J.* 2018;51(3):1702120.

38. Teo YJ, Ng SL, Mak KW, et al. Renal $CD169^{++}$ resident macrophages are crucial for protection against acute systemic candidiasis. *Life Sci Alliance.* 2021;4(5):e202000890.

39. Caslin HL, Bhanot M, Bolus WR, Hasty AH. Adipose tissue macrophages: unique polarization and bioenergetics in obesity. *Immunol Rev.* 2020; 295(1):101-113.

40. Yang S, Yuan H-Q, Hao Y-M, et al. Macrophage polarization in atherosclerosis. *Clin Chim Acta.* 2020;501:142-146.

41. Cailhier JF, Partolina M, Vuthoori S, et al. Conditional macrophage ablation demonstrates that resident macrophages initiate acute peritoneal inflammation. *J Immunol.* 2005;174(4):2336-2342.

42. Przybyla B, Gurley C, Harvey JF, et al. Aging alters macrophage properties in human skeletal muscle both at rest and in response to acute resistance exercise. *Exp Gerontol.* 2006;41(3):320-327.

43. Shi X, Shiao SL. The role of macrophage phenotype in regulating the response to radiation therapy. *Transl Res.* 2018;191:64-80.

44. Alvarez S, Boveris A. Mitochondrial nitric oxide metabolism in rat muscle during endotoxemia. *Free Radic Biol Med.* 2004;37(9):1472-1478.

45. MacMillan-Crow LA, Thompson JA. Tyrosine modifications and inactivation of active site manganese superoxide dismutase mutant (Y34F) by peroxynitrite. *Arch Biochem Biophys.* 1999;366(1):82-88.

46. Yamakura F, Matsumoto T, Fujimura T, et al. Modification of a single tryptophan residue in human Cu,Zn-superoxide dismutase by peroxynitrite in the presence of bicarbonate. *Biochim Biophys Acta.* 2001;1548(1):38-46.

47. Niles JC, Wishnok JS, Tannenbaum SR. Peroxynitrite-induced oxidation and nitration products of guanine and 8-oxoguanine: structures and mechanisms of product formation. *Nitric Oxide.* 2006;14(2):109-121.

48. Radi R, Cassina A, Hodara R, Quijano C, Castro L. Peroxynitrite reactions and formation in mitochondria. *Free Radic Biol Med.* 2002;33(11): 1451-1464.

49. Cai Z, Lin M, Wuchter C, et al. Apoptotic response to homoharringtonine in human wt p53 leukemic cells is independent of reactive oxygen species generation and implicates Bax translocation, mitochondrial cytochrome c release and caspase activation. *Leukemia.* 2001;15(4):567-574.

50. Ko CH, Shen S-C, Hsu C-S, Chen Y-C. Mitochondrial-dependent, reactive oxygen species-independent apoptosis by myricetin: roles of protein kinase C, cytochrome c, and caspase cascade. *Biochem Pharmacol.* 2005;69(6):913-927.

51. Seong M, Lee DG. Reactive oxygen species-independent apoptotic pathway by gold nanoparticles in *Candida albicans*. *Microbiol Res.* 2018;207: 33-40.

52. Ochoa CD, Wu RF, Terada LS. ROS signaling and ER stress in cardiovascular disease. *Mol Aspects Med.* 2018;63:18-29.

53. Di S, Fan C, Ma Z, et al. PERK/eIF-2α/CHOP pathway dependent ROS generation mediates butein-induced non-small-cell lung cancer apoptosis and G2/M phase arrest. *Int J Biol Sci.* 2019;15(8):1637-1653.

54. Lu H-L, Huang X-Y, Luo Y-F, Tan WP, Chen PF, Guo YB. Activation of M1 macrophages plays a critical role in the initiation of acute lung injury. *Biosci Rep.* 2018;38(2):BSR20171555.

55. Kim JJ, Lee SB, Park JK, Yoo YD. TNF-alpha-induced ROS production triggering apoptosis is directly linked to Romo1 and Bcl-X(L). *Cell Death Differ.* 2010;17(9):1420-1434.

56. Pronk CJH, Veiby OP, Bryder D, Jacobsen SEW. Tumor necrosis factor restricts hematopoietic stem cell activity in mice: involvement of two distinct receptors. *J Exp Med.* 2011;208(8):1563-1570.

57. Xue X, Piao J-H, Nakajima A, et al. Tumor necrosis factor α (TNFalpha) induces the unfolded protein response (UPR) in a reactive oxygen species (ROS)-dependent fashion, and the UPR counteracts ROS accumulation by TNFalpha. *J Biol Chem.* 2005;280(40):33917-33925.

58. Mertas A, Duliban H, Szliszka E, Machorowska-Pieniążek A, Król W. N-[3-(Aminomethyl)benzyl]acetamidine (1400 W) as a potential immunomodulatory agent. *Oxid. Med. Cell. Longev.* 2014;2014:491214.

59. Pereira PMR, Edwards KJ, Mandleywala K, et al. iNOS regulates the therapeutic response of pancreatic cancer cells to radiotherapy. *Cancer Res.* 2020;80(8):1681-1692.

60. Xu J, Luo Y, Yuan C, et al. Downregulation of nitric oxide collaborated with radiotherapy to promote anti-tumor immune response via inducing CD8+ T cell infiltration. *Int J Biol Sci.* 2020;16(9):1563-1574.

61. Wong JYC, Filippi AR, Dabaja BS, Yahalom J, Specht L. Total body irradiation: guidelines from the International Lymphoma Radiation Oncology Group (ILROG). *Int J Radiat Oncol Biol Phys.* 2018;101(3):521-529.